Chemical Engineering Journal 270 (2015) 572–581

Contents lists available at ScienceDirect

Chemical Engineering Journal

journal homepage: www.elsevier.com/locate/cej

Synergetic conditioning of sewage sludge via Fe^{2+}/persulfate and skeleton builder: Effect on sludge characteristics and dewaterability

Yafei Shi [a,1], Jiakuan Yang [a,*], Wenbo Yu [a], Shinan Zhang [a], Sha Liang [a,1], Jian Song [a], Qi Xu [a], Nan Ye [a], Shu He [b], Changzhu Yang [a], Jingping Hu [a]

[a] School of Environmental Science and Engineering, Huazhong University of Science and Technology, Wuhan 430074, China
[b] Universtar Science & Technology (Shenzhen) Co., Ltd., Shenzhen 518057, China

HIGHLIGHTS

- $Fe^{2+}/S_2O_8^{2-}$—phosphogypsum for sludge conditioning is firstly proposed.
- $SO_4^{\cdot-}$ was identified as the dominant radical by radical quenching experiment.
- $CaSO_4{\cdot}2H_2O$ could be newly generated and acted as an effective skeleton builder.
- The transforms of proteins and polysaccharides in floc were determined.
- The bound water was released and reduced significantly.

GRAPHICAL ABSTRACT

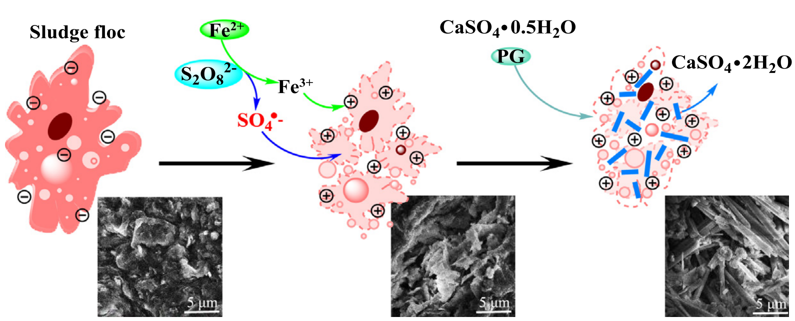

ARTICLE INFO

Article history:
Received 16 December 2014
Received in revised form 26 January 2015
Accepted 30 January 2015
Available online 18 February 2015

Keywords:
Sewage sludge
Chemical conditioning
Sulfate radical
Phosphogypsum
Extracellular polymeric substances (EPS)
Sludge dewatering

ABSTRACT

High water affinity of extracellular polymeric substances (EPS) and high compressibility of sewage sludge solids have negative impacts on sludge dewatering. In this study, a composite conditioner, Fe^{2+}–activated sodium persulfate (denoted as Fe^{2+}/SPS) combined with thermal–pretreated phosphogypsum (PG), was used to improve the sludge dewaterability. The mechanism of the composite conditioning of sewage sludge was elucidated: the proteins in tightly bound EPS were transferred into the filtrate and loosely bound EPS, and the polysaccharides in loosely and tightly bound EPS were transferred into the filtrate; the bound water was released and reduced from 2.60 g/g DS (dry solid) initially to 0.81 g/g DS; specific resistance to filtration and capillary suction time were reduced by 91.6% and 88.4%, respectively. Radical quenching experiment indicated that sulfate radical ($SO_4^{\cdot-}$) is the dominant free radical and plays an important role in determining the oxidation–reduction potential during conditioning. Moreover, both the XRD and SEM results clearly showed that Fe^{2+}/SPS combined with PG promoted the generation of column–shaped dihydrate gypsum in the conditioned sludge. Thus, the dihydrate gypsum crystals could act as skeleton builders, which create a more permeable and rigid lattice structure of the sludge cake. The improvement of sludge dewatering was confirmed by diaphragm filter press dewatering process, which yielded 45.7 wt% cake moisture content and 91.7% dewatering efficiency.

Abbreviations: AOPs, advanced oxidation processes; CST, capillary suction time; DS, dry solid; EPS, extracellular polymeric substances; LB–EPS, loosely bound–EPS; MIP, mercury intrusion porosimetry; ORP, oxidation–reduction potential; PG, phosphogypsum; PN, protein; PS, polysaccharides; RS, raw sludge; SF, $Fe^{2+}/S_2O_8^{2-}$; SFP, $Fe^{2+}/S_2O_8^{2-}$–PG; SPS, sodium persulfate; SRF, specific resistance to filtration; TBA, tert–butyl alcohol; TB–EPS, tightly bound–EPS; TSS, total suspended solids; VSS, volatile suspended solids.

* Corresponding author. Tel.: +86 27 87792102; fax: +86 27 87792101.
E-mail address: jkyang@mail.hust.edu.cn (J. Yang).

[1] These two authors contributed equally to this paper.

http://dx.doi.org/10.1016/j.cej.2015.01.122
1385-8947/

1. Introduction

Sewage sludge is a by–product produced in wastewater treatment facilities, and the treatment and disposal of sewage sludge introduces significant costs to the operation of these facilities [1]. Dewatering is an important process for sludge treatment and disposal. Commonly, difficulties in sludge dewatering can be attributed to its highly compressible nature, high organic content, and abundance of colloids [2,3]. In order to reduce the compressibility of the sludge solids or rupturing extracellular polymeric substances (EPS), numerous researches on conditioning processes have been illustrated to improve sludge dewaterability, such as physical [4], chemical [2,4], thermal [5], and biological [6] processes. Advanced oxidation processes (AOPs) are considered to be effective pretreatment for sludge conditioning. Fenton and Fenton–like processes, as part of the AOPs family, are commonly used for sludge dewatering [7–10]. Mustranta and Viikari [11] reported that H_2O_2 with a concentration of 15–30 mmol/L was effective to decrease the specific resistance to filtration (SRF) values to a low level at 70 °C with a reaction time of 1–2 h at pH of 3. Unfortunately, the drawbacks of the classic Fenton oxidation is limited by drawbacks including potential safety hazards associated with the use of H_2O_2 and requirement of pH lowering to 2.5–3, followed by a subsequent neutralization [12].

In recent years, activated persulfate receives much attention as an alternative oxidant ($E° = 2.01$ V) with its non–selective reactivity and good chemical stability under room temperatures. It can initiate a free radical pathway through the formation of sulfate radicals ($E° = 2.6$ V) activated by heat, UV or transition metal. The reactions between persulfate and Fe^{2+} are shown in the following equations [13]:

$$S_2O_8^{2-} + 2Fe^{2+} \rightarrow 2Fe^{3+} + 2SO_4^{2-} \quad (k = 3.1 \times 10^4\ M^{-1}\ s^{-1}) \tag{1}$$

through the following steps:

$$S_2O_8^{2-} + Fe^{2+} \rightarrow Fe^{3+} + SO_4^{\cdot-} + SO_4^{2-} \quad (k = 2.0 \times 10^1\ M^{-1}\ s^{-1},\ 22\,°C) \tag{1-1}$$

$$SO_4^{\cdot-} + Fe^{2+} \rightarrow SO_4^{2-} + Fe^{3+} \quad (k = 4.6 \times 10^9\ M^{-1}\ s^{-1},\ 22\,°C,\ pH = 3\text{—}5) \tag{1-2}$$

when $SO_4^{\cdot-}$ serves as an oxidant and results in the formation of sulfate anion:

$$SO_4^{\cdot-} + e^- \rightarrow SO_4^{2-} \quad (E° = 2.6\ V) \tag{2}$$

$$\text{all pHs}: SO_4^{\cdot-} + H_2O \rightarrow SO_4^{2-} + HO^{\cdot} + H^+ \quad (k(H_2O) < 2 \times 10^3\ M^{-1}\ s^{-1}) \tag{3}$$

$$\text{alkaline pH}: SO_4^{\cdot-} + OH^- \rightarrow SO_4^{2-} + HO^{\cdot} \quad (k = 1.4\text{—}7.3 \times 10^7\ M^{-1}\ s^{-1}) \tag{4}$$

Interestingly, $Fe^{2+}/S_2O_8^{2-}$ has a good oxidant effect in a wider range of pH from 2 to 10, which makes it applicable in sludge conditioning. A couple of studies reported that the $Fe^{2+}/S_2O_8^{2-}$ might be an energy–efficient alternative oxidant for sludge conditioning. Zhen et al. [14,15] have shown an improved dewatering performance using $Fe^{2+}/S_2O_8^{2-}$ at higher dosages (i.e., $S_2O_8^{2-}$ 1.2 mmol/g volatile suspended solids (VSS) and Fe^{2+} 1.5 mmol/g VSS). Our previous study has shown $Fe^{2+}/S_2O_8^{2-}$ to be effective in improving the dewaterability with a 89.0% reduction in SRF and 84.1% in capillary suction time (CST), and achieving 52.6 wt% cake moisture content with a diaphragm filter press [16]. Although $Fe^{2+}/S_2O_8^{2-}$ yields a high dewatering efficiency, the high operating cost limits its practical application.

Physical conditioners, often referred to as skeleton builders, are effective to reduce the compressibility of sludge, because they could form a permeable and rigid lattice structure in sludge cake under high pressures. Some cheaper and easily available solid materials have been investigated as skeleton builders, such as fly ash, lime [17], wood chips and wheat dregs [18], gypsum [19], lignite [20], and tannery sludge incineration slag [21]. However, according to previous researches, very high dosages of skeleton builders could increase sludge volume and weight, which exerts significant adverse influence on the subsequent sludge transportation and disposal (e.g., landfill or incineration).

Either $Fe^{2+}/S_2O_8^{2-}$ reagents as AOPs reagents or physical conditioners as skeleton builders have been separately investigated in sewage sludge conditioning. Separate applications of two conditioners have been limited because of the shortcomings mentioned previously. Synergetic conditioning of sewage sludge with $Fe^{2+}/S_2O_8^{2-}$ and skeleton builder has not been reported in the literature. In this study, thermal–pretreated phosphogypsum (PG) was used as a novel skeleton builder since it has a different mineral phase of hemihydrate gypsum ($CaSO_4{\cdot}0.5H_2O$) when compared with natural gypsum with dihydrate phase ($CaSO_4{\cdot}2H_2O$) used in the literature [19]. Moreover, waste PG is a by–product in phosphorus chemical industry. In China, reuse of waste PG only accounts for less than 10% of total production, so PG is a cheap and readily available inorganic material which can be used as skeleton builder in most of the provinces of China. The schematic of this study is depicted in Fig. 1. After the conditioning of sewage sludge with $Fe^{2+}/S_2O_8^{2-}$ combined with thermal–pretreated PG, the effect of $Fe^{2+}/S_2O_8^{2-}$–PG conditioning on dewatering by a diaphragm filter press process was investigated.

2. Material and methods

2.1. Materials

Waste sewage sludge sample was a mixture of primary and secondary sludge taken from the Longwangzui wastewater treatment plant, Wuhan, China. Municipal wastewater of 150,000 m^3/d was treated by an anaerobic–anoxic–oxic process in this plant. The sample contains 96.65 wt% water with pH of 7.1 and soluble chemical oxygen demand of 831.1 mg/L. Table 1 presents some characteristics of this raw sludge (RS). To obtain a good reproducibility, all the tests were completed within 3 d and the sludge was stored at 4 °C.

Sodium persulfate (SPS) ($Na_2S_2O_8$, purity >99.9%) and ferrous sulfate ($FeSO_4{\cdot}7H_2O$, purity >99.9%) were analytical reagents

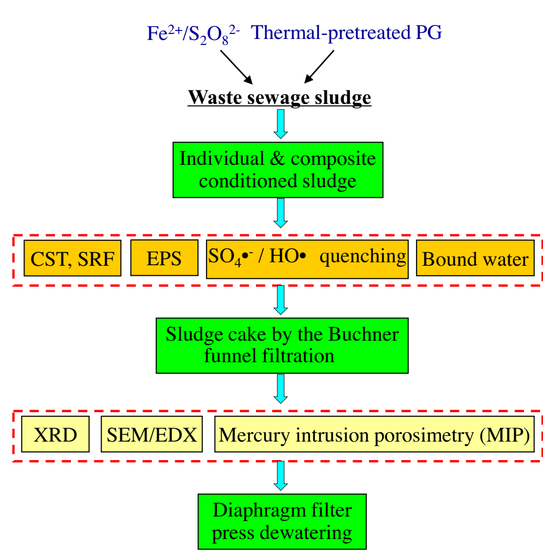

Fig. 1. The schematic of the study.

Table 1
Characteristics of the RS sample.

pH	Water content (wt%)	SCOD (mg/L)	TSS (g/L)	VSS/TSS (%)	SRF ($\times 10^{13}$ m/kg)	CST (s L/g TSS)
7.1	96.65	831.1	35.0	50.8	1.62	5.2

Table 2
Chemical compositions of raw PG (wt%).

SiO_2	Al_2O_3	Fe_2O_3	CaO	MgO	SO_3	F	P_2O_5	[a]LOI
6.25	0.43	0.13	28.64	0.17	40.21	0.23	1.84	21.69

[a] LOI = loss of ignition at 1200 °C.

(Sinopharm company, Shanghai, China). The dissolved Fe^{2+} solutions were prepared from $FeSO_4{\cdot}7H_2O$ in ultrapure water. Raw PG was collected from a phosphate fertilizer company in Guangxi, China. Prior to being used as the skeleton builder, the thermal–pretreated PG was sieved with a mesh size of 0.08 mm after 150 °C for 2 h. The chemical compositions of the waste PG are given in Table 2.

2.2. Conditioning test

Jar tests for the sludge conditioning experiment were conducted using a programmable jar test apparatus. Table 3 tabulates the details of the experimental procedures of individual or combined conditioning. The $Fe^{2+}/S_2O_8^{2-}$–PG (denoted as SFP) conditioning was conducted as follows. First, SPS was added at a dose of 100 mg/g DS (dry solid) to a 300–mL sludge sample in a 500–mL beaker and stirred at 300 rpm for 10 min. Afterwards, 23.5 mg Fe^{2+}/g DS was sequentially added and stirred at 150 rpm for 15 min. It is necessary to slow down or control the reaction to avoid the rapid conversion of Fe^{2+} to Fe^{3+} by the $SO_4^{\cdot-}$ as shown in Eqs. (1-1) and (1-2). Last, thermal–treated PG of 300 mg/g DS was added and the mixture was stirred at 150 rpm for 5 min. SPS (denoted as S), Fe^{2+} (denoted as F), PG (denoted as P), or Fe^{2+}/SPS (denoted as SF) was also added to sludge as the control in Table 3. All the conditioning processes were conducted at the identical stirring speed for identical time to ensure identical mechanical mixing effect.

After conditioning, 100 mL conditioned sludge sample was poured into a 9–cm standard Buchner funnel fitted with pre–wetted 0.45 μm filter paper, and then a constant vacuum pressure of 80 kPa was applied until no filtrate coming out. Both the filtrate volume and the sludge cake weight were recorded. The sludge cake samples were used in X–ray powder diffraction (XRD), scanning electron microscopy–energy dispersive X–ray spectroscopy (SEM–EDX), and mercury intrusion porosimetry (MIP) analyses.

2.3. Radical quenching experiment

To evaluate the contributions of free radicals generated during the conditioning, quenching studies were conducted by adding ethanol or tert–butyl alcohol (TBA) to identify the dominant effective radicals. The reaction rate constant of ethanol with $HO^{\cdot}$ is approximately $(1.2–2.8) \times 10^9$ mol/L s, which is about 15–140 times higher than with $SO_4^{\cdot-}$, about $(1.6–7.7) \times 10^7$ mol/L s. In contrast, the reaction rate constant of TBA with $HO^{\cdot}$ is approximately $(3.8–7.6) \times 10^8$ mol/L s, which is about 400–1900 times higher than with $SO_4^{\cdot-}$, about $(4.0–9.1) \times 10^5$ mol/L s. In general, the reaction rate constant of $SO_4^{\cdot-}$ with ethanol is about 1000 times higher than with TBA. Therefore, ethanol and TBA were used to quench the relevant radicals in this experiment. These radical quenching experiments were designed to identify whether sulfate radical ($SO_4^{\cdot-}$) or hydroxyl radical ($HO^{\cdot}$) is the dominant free radical in $Fe^{2+}/S_2O_8^{2-}$–PG conditioning of sewage sludge. Three sets of quenching experiments were conducted: (1) addition of ethanol followed by SFP conditioning, denoted as ethanol–SFP; (2) addition of TBA followed by SFP conditioning, denoted as TBA–SFP; (3) addition of both ethanol and TBA followed by SFP conditioning, denoted as ethanol–TBA–SFP. The molar ratio of the radical quenching agents to SPS was 50:1. The conditioning parameters were the same as described previously in Section 2.2. The CST values were measured before and after each addition. Moreover, the oxidation–reduction potential (ORP) was determined by using an online ORP–2096–meter (Shanghai Boqu Instrument Co., Shanghai, China).

2.4. Dewatering test

Dewatering tests were performed using a laboratory–scale diaphragm filter press with six diaphragm plates (250 mm × 250 mm, 10 mm depression). Two different conditioning agents were used: (1) SF: 23.5 mg Fe^{2+}/g DS, and 100.0 mg SPS/g DS; (2) SFP: 23.5 mg Fe^{2+}/g DS, 100.0 mg SPS/g DS, and 259.0 mg PG/g DS. In addition, the raw sludge without any conditioning agents served as a control. The dewatering process is divided into two stages, feed and compression stage respectively. Detailed descriptions of the procedure are provided in Supplementary material. The moisture content of filter cake was measured and dewatering efficiency was calculated according to Eq. (5):

$$\text{Dewatering efficiency } (\%) = \frac{M_{\text{filtrate}} - M_{\text{conditioners}}}{M_{\text{conditioned sludge}}} \times 100 \quad (5)$$

where M_{filtrate} is the mass of water in filtrate, $M_{\text{conditioners}}$ is the mass of water in the conditioners, and $M_{\text{conditioned sludge}}$ is the total mass of water in conditioned sludge used for dewatering.

2.5. Analytical methods

2.5.1. CST and SRF

Both CST and SRF values were measured to evaluate the sludge dewaterability in this study. The CST was measured using a 304M CST instrument (Triton, UK) equipped with a 10 mm diameter funnel. The CST values were normalized by dividing them with the initial TSS concentration and then expressed in units of seconds liter per gram TSS (s L/g TSS) [22]. The SRF values were obtained using

Table 3
Details of the experimental procedures of single and composite conditionings.

Symbol	RS and conditioned sludge	Dosage (mg/g DS)			Conditioning procedures
		SPS	[a]Fe^{2+}	PG	
RS	RS	0	0	0	300 rpm for 10 min → 150 rpm for 15 min
S	SPS	100	0	0	Add SPS → 300 rpm for10 min → 150 rpm for 15 min
F	Fe^{2+}	0	23.5	0	300 rpm for 10 min → add Fe^{2+} solutions → 150 rpm for 15 min
P	PG	0	0	300	300 rpm for 10 min → 150 rpm for 10 min → add PG → 150 rpm for 5 min
SF	Fe^{2+}/SPS	100	23.5	0	Add SPS → 300 rpm for 10 min → add Fe^{2+} solutions → 150 rpm for 15 min
SFP	Fe^{2+}/SPS–PG	100	23.5	300	Add SPS → 300 rpm for 10 min → add Fe^{2+} solutions → 150 rpm for 10 min → add PG → 150 rpm for 5 min

[a] Sequential dosing of Fe^{2+} solution with a 1/3 increment of total dosage per 5 min.

the method described by Liu et al. [10]. The SRF reduction efficiency and CST reduction efficiency were also calculated.

2.5.2. Extraction and determination of EPS

A two–layer model for the structure of bound EPS was used to evaluate the effects of conditioning on EPS, namely as tightly bound EPS (TB–EPS) and loosely bound EPS (LB–EPS). The first layer consists of TB–EPS, which is bound tightly and stably to the cell surface. The second layer consists of LB–EPS, which is a loose slim layer without an obvious edge [3]. A modified heat extraction method was used to extract the LB–EPS and TB–EPS from the sludge, typically following by the procedures of Li et al. [23]. The proteins (PN) was analyzed by the modified Lowry method using bovine serum albumin as the standard [24]. The polysaccharides (PS) content was tested with the anthrone method by using glucose as the standard [25]. All of these batch experiments were carried out in duplicate.

2.5.3. Bound water content

A differential scanning calorimetry (DSC) method was employed to measure the bound water content [26,27]. The apparatus used in this study was a Diamond DSC analyzer (PerkinElmer Inc., USA) equipped with a liquid nitrogen cooling system. To achieve uniform sample, the sludge was first centrifuged at 1000 rpm for 10 min to remove most of the free water. Approximately 20 mg sample was first subjected to a temperature of −25 °C, assuming that all free water was converted to ice under this condition, and then heated back to 25 °C at a heating rate of 2 °C/min. After that, the sample was frozen back to −25 °C at a freezing rate of −2 °C/min. The thermograms of the raw and conditioned sludge are provided in Supplementary material. Thus, the amount of free water could be determined by the respective areas of the endothermic curve and the exothermic curve as in Eq. (6):

$$FW = K \times A \tag{6}$$

where FW is the mass of free water (mg), A is the area of the exothermic curve (mJ), and K is the conversion factor (mg/mJ), determined from obtaining the thermograms of pure water of known mass. K was calculated to be 0.0031 mg/mJ for pure water with four different masses by Zhang et al. [28].

The bound water was determined as the difference between the known total water of the sludge sample and the mass of free water.

2.5.4. Mercury intrusion porosimetry of sludge cake

Mercury intrusion porosimetry (MIP) tests were performed on the filter cakes of RS, SF, P and SFP conditioned sludge to determine the average cake porosity by using a commercial mercury porosimeter (AutoPore IV 9500, Micromeritics Instrument Co., USA). The cakes were dried in an oven at 45 °C for 24 h prior to the porosimetry tests. The maximum pressure applied in the high–pressure cycle was 228 MPa.

2.5.5. Mineral phases and microstructural characteristics of sludge cake

Mineral phases of sludge cakes were analyzed by XRD techniques (X'Pert Pro, PANalytical B.V., Holland) with 40 kV acceleration voltage with Ni–filtered Cu Kα radiation. XRD spectra were acquired with scanning rate of 0.2785°/s for 2θ in the range from 5° to 75°. Microstructural characteristics analyses of freeze–dried sludge were carried out with a SEM–EDX (Nova NanoSEM 450, FEI, Netherlands) operated at 10 kV of acceleration voltage, and the samples were coated with Au prior to the characterization.

3. Results and discussion

3.1. Effects of single and composite conditioning on sludge characteristics

3.1.1. Dewaterability

There were notable differences in SRF and CST under various conditioning experiments shown in Fig. 2.

As shown in Fig. 2a and b, the individual addition of SPS, Fe^{2+}, and PG could hardly improve the performance of sludge dewatering. Interestingly, SPS could result in higher reduction of SRF and CST than those of Fe^{2+} or PG only. It is most likely due to the SPS self–decomposition or being activated by other substances present in the aqueous sludge solution. This result is in accordance with the results of Liang et al. [29], who demonstrated that the decomposition of persulfate was partially induced by soil minerals rather than by ferrous ions in the soil slurry mixture.

Moreover, a synergetic effect was observed, in which the reductions of SRF and CST of SF conditioning are higher than the sum of the individual ones. As shown in Fig. 2, the SRF values of sludge samples conditioned with SF were rapidly decreased from initial 1.67×10^{13} to 0.15×10^{13} m/kg and the CST values also decreased from 5.2 to 0.8 s L/g TSS. On the other hand, SFP conditioning further reduced the SRF and CST to 0.14×10^{13} m/kg and 0.6 s L/g TSS, respectively. This improvement is plausibly resulted from the breakdown of sludge flocs and the formation of skeleton structures that are more prone to quick dewatering.

3.1.2. EPS and bound water content

Proteins and polysaccharides are the principal component of the EPS matrix in the activated sludge. Fig. 3 shows the changes of protein and polysaccharide contents in the filtrate, LB–EPS, and TB–EPS, respectively.

Considerable solubilization of proteins and polysaccharides was found in filtrate after conditioning and is probably attributable to the cell disruption. As shown in Fig. 3a, after SF and SFP

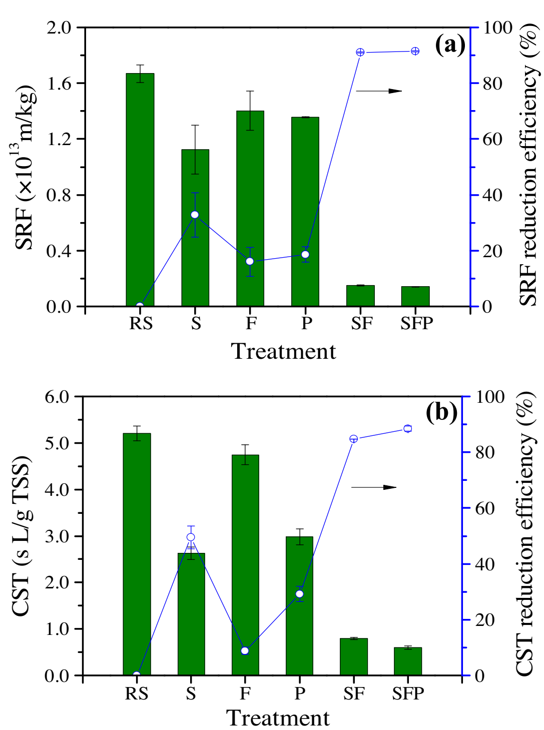

Fig. 2. Effects of different conditionings on the dewaterability: (a) SRF, and (b) CST.

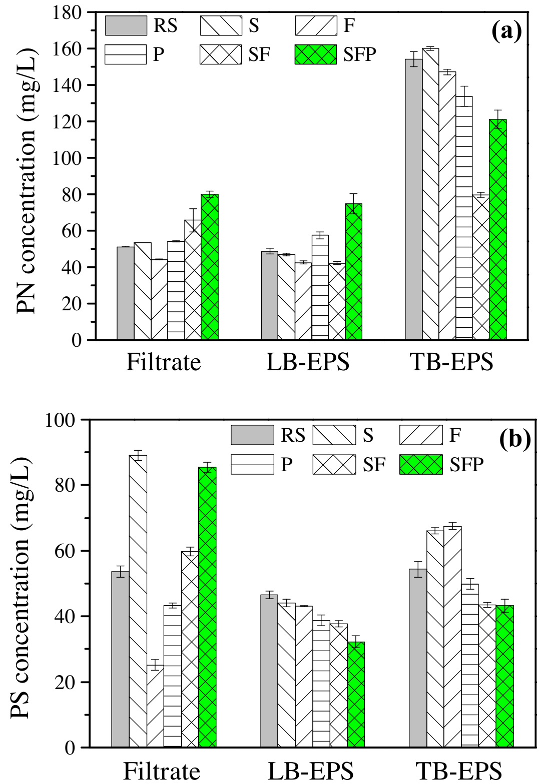

Fig. 3. Effects of different conditionings on (a) PN and (b) PS in filtrate, LB–EPS, and TB–EPS.

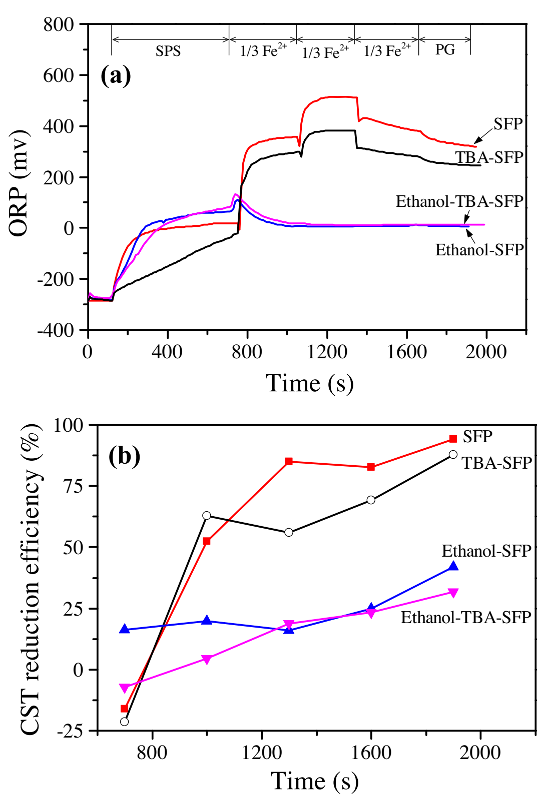

Fig. 4. Influences of ethanol and TBA on (a) ORP and (b) CST of the conditioned sludges.

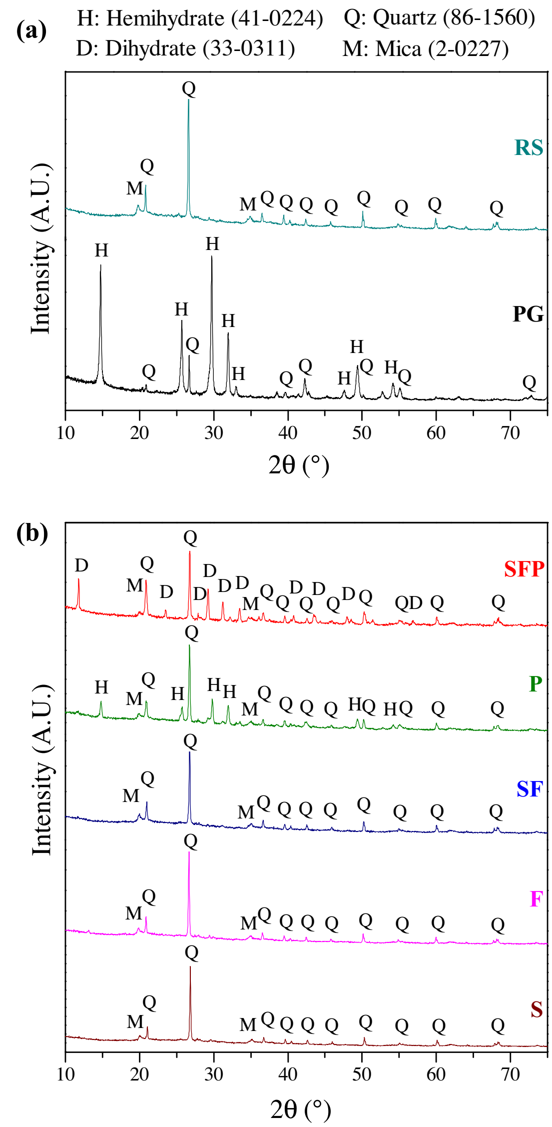

Fig. 5. The XRD patterns of (a) the raw sludge and thermal–pretreated PG, and (b) the conditioned sludges.

conditioning, the proteins in both filtrate and LB–EPS were increased; however, it in TB–EPS was decreased. It indicated that the proteins in TB–EPS were transferred into the filtrate and LB–EPS. Furthermore, Fig. 3b indicates that the polysaccharides in filtrate significantly increased when compared with RS, while the polysaccharides in both LB– and TB–EPS significantly decreased after SF and SFP conditioning. It indicated that the polysaccharides in LB– and TB–EPS were transferred into the filtrate. For example, compared with RS, the proteins in LB–EPS and TB–EPS decreased by 13.4% and 48.3% after the SF conditioning, respectively, while increased by 28.3% in the filtrate. In contrast, the polysaccharides in LB–EPS and TB–EPS decreased accordingly by 18.8% and 19.9%, while increased by 11.4% in the filtrate. In general, SFP conditioning caused more proteins in the LB–EPS and more polysaccharides in the filtrate than those after SF conditioning. The proteins increased by 53.4% in LB–EPS, while the proteins and polysaccharides decreased by 21.3% and 20.4%, in TB–EPS, respectively.

The enhanced dewaterability by SFP conditioning could be attributed to the fact that sulfate radical first breaks up the outer region of flocs and then consumes its release of organic substances. The breakup of outer region also help to destroy the inner flocs,

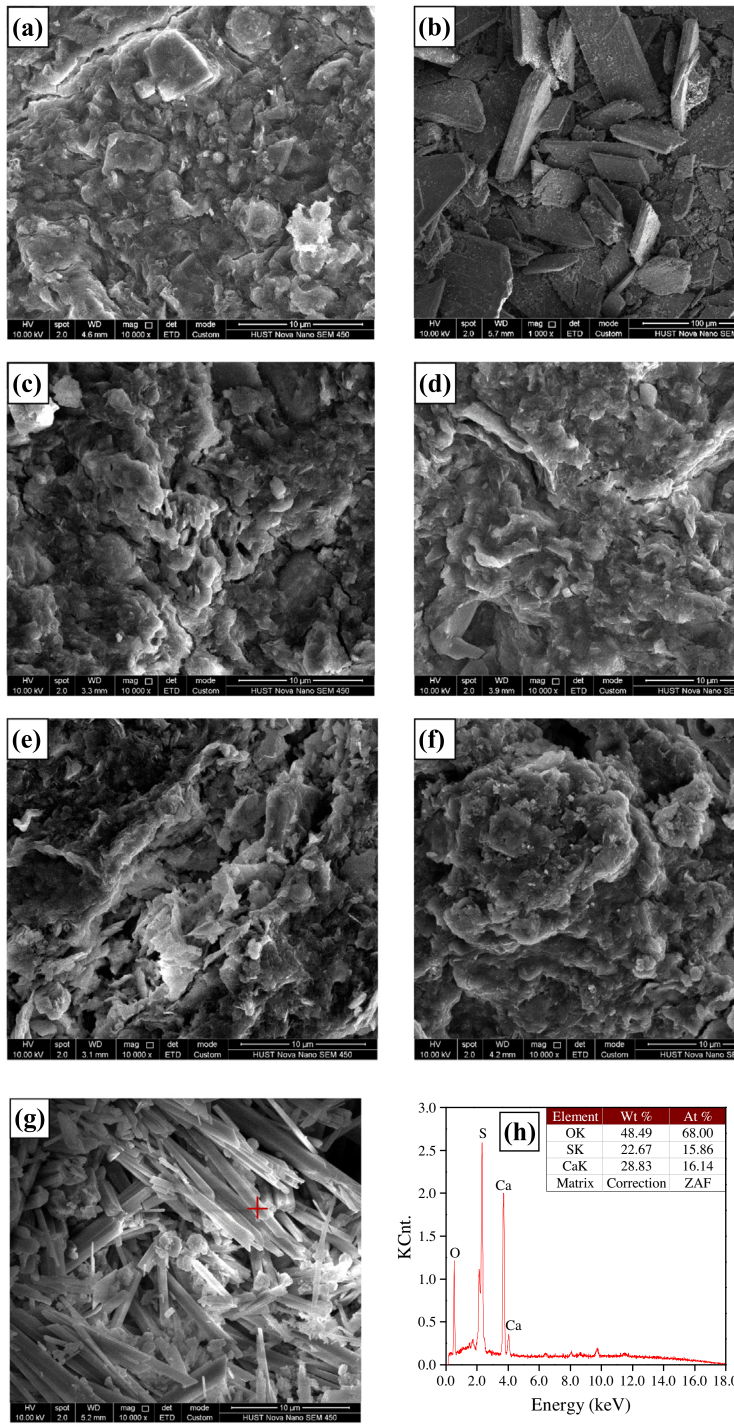

Fig. 6. The SEM images of the filter cake after different conditionings: (a) raw sludge, (b) thermal–pretreated PG, (c) S, (d) F, (e) SF (f) P, (g) SFP, and (h) EDX spectra of the filter cake of SFP.

which induced the rise of protein and polysaccharides in filtrate. This is a synchronized process of ''degradation'' and ''generation''. As a result, a large quantity of EPS–bound water and interstitial water was released into the free water. The bound water content decreased from initial 2.60 g/g DS of raw sludge to 1.01 g/g DS after SF conditioning, and further decreased to 0.81 g/g DS by SFP conditioning. A large number of bound water in the flocs resulted in difficulty of solid–liquid separation; however, after SF conditioning, 61.1% of the bound water was released. With the addition of pretreated PG, the bound water content was further reduced by 68.9%. It is concluded that bound water can be released from the destructed EPS after the Fe^{2+}/SPS oxidation. In addition, osmotic effect might also contribute to the release of bond water [2]. The existence of cations (Na^{+}, Fe^{2+}, Fe^{3+}, and Ca^{2+}) increases the ionic strength of the bulk solution and thus decreases the chemical potential of water in the inter–floc region [30].

3.1.3. ORP and radical identification

To identify the dominant radical species formed in SFP conditioning, the variations of the ORP and corresponding CST were investigated in the presence of ethanol or TBA as shown in Fig. 4.

Variations in ORP values under four different experimental conditions are presented in Fig. 4a. It was observed that the ORP values are significantly reduced in the presence of ethanol or ethanol–TBA after Fe^{2+} addition. The ORP curve of ethanol–SFP is close to the ORP curve of ethanol–TBA–SFP. However, the ORP values of ethanol–SFP and ethanol–TBA–SFP are apparently less than those of SFP and TBA–SFP.

As it can be seen in Fig. 4b, significant drop in CST reduction efficiency was observed when ethanol or TBA was present. It has been found that the CST reduction efficiency of SFP (94.0%) and TBA–SFP (87.7%) changes to 42.0% and 31.7% in the ethanol–SFP and ethanol–TBA–SFP systems, respectively. CST reduction efficiency in ethanol–SFP is close to that of ethanol–TBA–SFP, and CST reduction efficiency in SFP is closer to that of TBA–SFP. However, CST reduction efficiency in ethanol–SFP and ethanol–TBA–SFP are apparently less than those of SFP and TBA–SFP, which is consistent with the influence on ORP in Fig. 4a.

From Eqs. (1)–(4), both $SO_4^{\cdot-}$ and $HO^{\cdot}$ possibly exist in the Fe^{2+}/SPS system. In literature, there is no report on the dominant radical species in the sewage sludge conditioning system with Fe^{2+}/SPS. As shown in Fig. 4b, CST reduction efficiency in SFP is close to that of TBA–SFP. It implies that hydroxyl radical is not the dominant radical in SFP conditioning system since TBA mainly reacts with hydroxyl radical. Furthermore, CST reduction efficiency in ethanol–SFP and ethanol–TBA–SFP are apparently less than those of TBA–SFP. It implies that $SO_4^{\cdot-}$ is the dominant radical in SFP conditioning system since previous study have shown that ethanol is a well–known quenching agent for both hydroxyl and sulfate radicals [31]. Therefore, the results suggest that $SO_4^{\cdot-}$ play a dominant role in the advanced oxidation in SFP conditioning system for sewage sludge at neutral pH. These observations are in agreement with the results reported by Liang and Su [32].

3.1.4. Mineral phases and microstructure

The XRD patterns of the raw sludge and the thermal–pretreated PG are shown in Fig. 5a. As shown in this figure, the dominant mineral phases of the raw sludge are quartz (SiO_2) and mica (K–Mg–Fe–Al–Si–O–H_2O), which originate from the inorganic material in sewage sludge. The major mineral phase of the thermal–pretreated PG is hemihydrate gypsum ($CaSO_4{\cdot}0.5H_2O$), with small amount of inert impurity of quartz, which is consistent with the results of Yang et al. [33].

The XRD patterns of the conditioned sludge with various conditioners (labeled as S, F, SF, P and SFP) are shown in Fig. 5b. As shown in this figure, quartz and mica are identified in the conditioned sludge cakes of S, F, and SF. It is interesting to note that $CaSO_4{\cdot}0.5H_2O$ is identified in the conditioned sludge of P and the thermal–pretreated PG. However, dihydrate phase ($CaSO_4{\cdot}2H_2O$) is identified in the conditioned sludge of SFP, instead of $CaSO_4{\cdot}0.5H_2O$ in the thermal–pretreated PG. This phenomenon was attributed to the fact that there are crystal habit modifier and salt, such as Fe^{3+}, Ca^{2+}, and SO_4^{2-} in the SFP conditioning system, which could promote the formation of $CaSO_4{\cdot}2H_2O$. These findings were in good agreement with findings of Abdel–Aal et al. [34] that the higher concentration of Ca^{2+} and SO_4^{2-} ions caused higher inter–ionic attractions and accelerated the nucleation rates, resulting in an increase in crystals and on growth rate of already formed crystals.

Fig. 6 presents the SEM images of the filter cake after different conditionings. As shown in Fig. 6a, a relatively dense structure is

Table 4
Pore size distribution of the conditioned sludge and RS.

Sample	Total pore volume (mL/g)	Median pore diameter (μm)	Porosity (%)
RS	0.052	0.01	8.1
SF	0.104	0.02	15.2
SFP	0.157	1.29	17.0

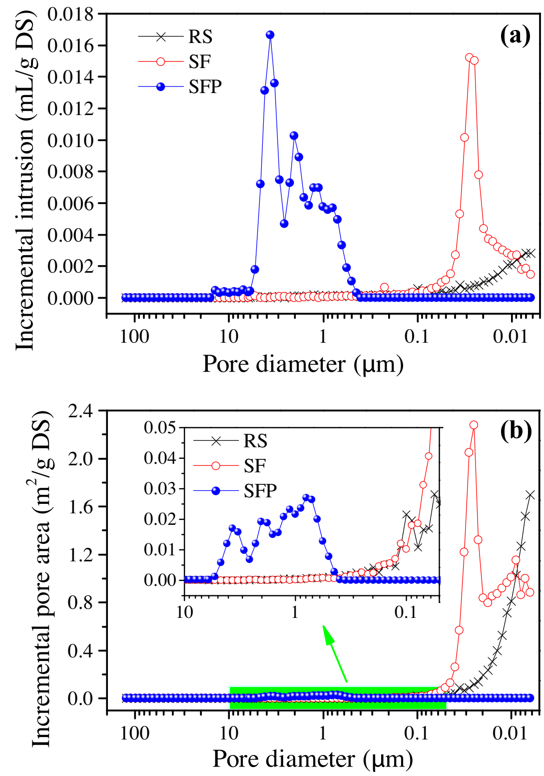

Fig. 7. Mercury intrusion porosity acted as a function of void volume per mass of total solids: (a) pore diameter versus incremental intrusion, (b) pore diameter versus incremental pore area.

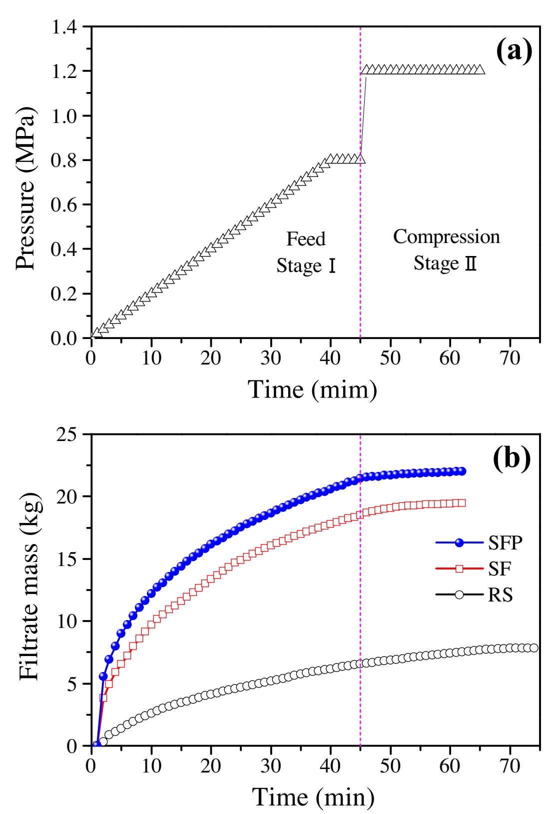

Fig. 8. Results of diaphragm filter pressing test: (a) the plot of the feed pressure versus time, (b) the plot of the total filtrate mass versus time.

found in raw sludge. Fig. 6b shows a plate–like structure for the PG sample pretreated at 150 °C. As shown in Fig. 6c, d, and f, the morphologies of filter cake have no significant changes, when compared to raw sludge after individual conditioners of S, F, or P. However, the morphology of sludge flocs revealed obviously more porous or lamellar structure when SF conditioning, as shown in Fig. 6e. Moreover, numerous column–shaped crystals are observed in the filter cake when Fe^{2+}/SPS–PG was used for the composite SFP conditioning, as shown in Fig. 6g. EDX spectra of the column–shaped crystal showed that the generated crystals were composed of S, Ca, and O, which are major elements of gypsum. Combined with the XRD patterns in Fig. 5, it indicated that the column–shaped crystal in SFP filter cake is $CaSO_4{\cdot}2H_2O$.

In summary, it is reasonable to believe that synergistic effect has actually occurred in the Fe^{2+}/SPS–PG conditioning system. With SFP conditioning, a large number of column–shaped crystals of $CaSO_4{\cdot}2H_2O$ generated from plate–shaped $CaSO_4{\cdot}0.5H_2O$ in the thermal–pretreated PG, which fills the sludge flocs and increases the porosity of the sludge cake.

3.2. Pore size distribution

MIP tests were performed on the dried sludge cakes. The results are shown in Table 4 and Fig. 7.

As shown in Table 4, the total pore volume, median pore diameter and porosity increased observably after SF and SFP conditioning. It is consistent with the morphologies observed in SEM images in Fig. 7. The total pore volume of raw sludge was 0.052 mL/g, and its median pore diameter and porosity was 0.01 μm and 8.1%, respectively. After SF conditioning, the total pore volume of SF was 0.104 mL/g, and its median pore diameter and porosity was 0.02 μm and 15.2%, respectively. It can be inferred that some pores or channels were created in the filtrated cake after Fe^{2+}/SPS oxidation. Furthermore, after SFP conditioning, the total pore volume of SFP was 0.157 mL/g, and its median pore diameter and porosity was 1.29 μm and 17.0%, respectively. Moreover, the SFP–sludge had a higher porosity than the SF–sludge, which further confirmed that a synergistic effect has actually occurred in the SFP conditioning system.

From the results in Fig. 7a, it is apparent that SFP conditioned sludge shows a broadly distributed pore diameters in the range of 0.4–6.0 μm, which is classified as macropore. Whereas for SF, pore diameters are a narrowly distributed in the smaller range of around 0.01–0.05 μm, which is classified as mesopore. In comparison, pore diameters of RS sample are too small (<0.01 μm, mesopore and micropore) to be measured precisely. It can be concluded the fact that the SFP generates column–shaped dihydrate phase, which contributes to a broad distribution of pore sizes, and thus increases total pore volume and porosity.

Fig. 7b depicts the relationship between incremental pore area and pore diameter. The incremental pore area of SFP sludge is mainly distributed at the pore diameter range of 0.5–6 μm. In contrast, the incremental pore areas of the conditioned sludge cake of RS and SF are mainly distributed at the pore diameter of 0.05 μm or less. The smaller pore diameter, the more incremental pore area is. In the conditioned sludge cakes of RS and SF, large quantities of mesopores and micropores increase the pore area, which contributes to the enchantment of moisture adsorption capacity. However, in the

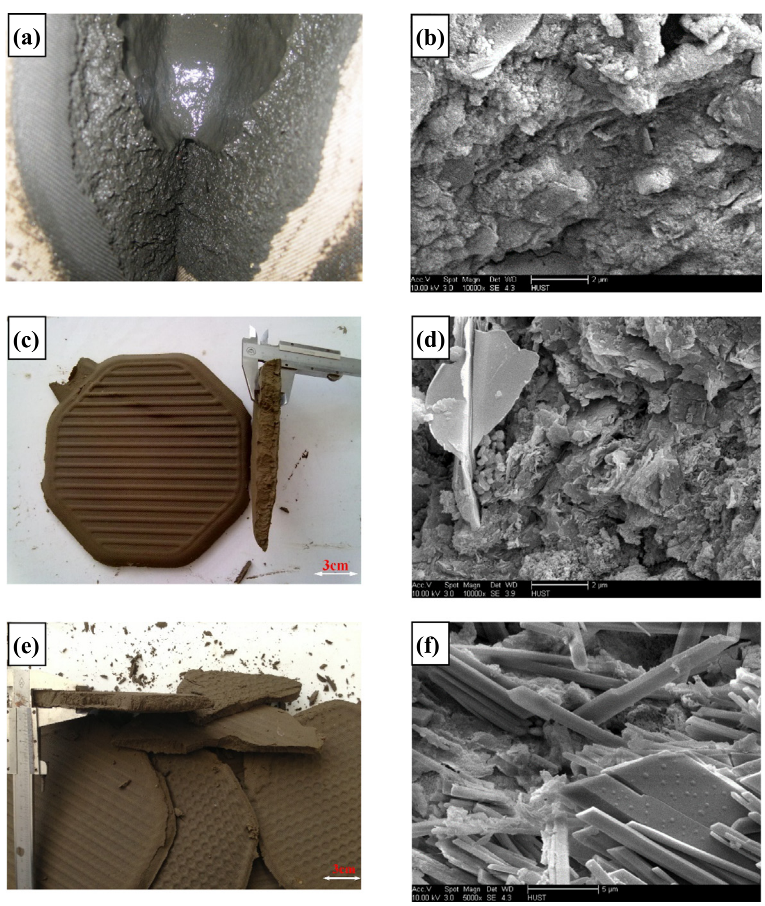

Fig. 9. The photos of the dewatered sludge cake: (a) raw sludge without any conditioner, (c) SF conditioning, and (e) SFP conditioning; and SEM images of the dewatered sludge cake: (b) raw sludge without any conditioner, (d) SF conditioning, and (f) SFP conditioning.

conditioned sludge cake of SFP, plenty of macropores and through–holes increase the water pore channel, which contributes to improvement of dewaterability of the conditioned sludge.

3.3. Dewatering performance

All the diaphragm filter dewatering experiments were carried out using the same feed pressure procedure, as shown in Fig. 8a. Both the total filtrate mass and the filtration rate after SFP conditioning are significantly higher than those of SF conditioning, especially within the first 10 min of the pressing process (Fig. 8b).

As shown in Fig. 9a, it was difficult to obtain a successful dewatered cake if raw sludge was directly fed into the diaphragm filter without any conditioner, even after a long dewatering time. In Fig. 9c and e, the dewatered cakes with a good shape were observed after the SF and SFP conditioning, respectively. The moisture contents of the dewatered sludge cakes after the SF and SFP conditioning were low, at 55.8 wt% and 45.7 wt%, respectively. Moreover, the dewatering efficiencies were high, at 89.5% and 91.7%, respectively, when compared to the 66.4% in raw sludge dewatering.

The SEM images of the dewatered sludge cake are shown in Fig. 9b, d and f. As shown in Fig. 9b, the morphology of the dewatered sludge from raw sludge appears as a dense and compact structure. In Fig. 9d, the morphology of SF dewatered sludge cake shows a fractal and pore structure. However, many regular column–shaped crystals is present in the microstructure of the SFP dewatered cake (Fig. 9f), which could be acted as a more rigid lattice, high porosity and permeability during filtration.

Last, it should be noted that Fe^{2+}/SPS–PG compounds contain sulfur S and thus the final conditioned sludge would present a high concentration of sulfur, indicating that although S is not a hazardous element, the dewatered cake is not very suitable for incineration disposal. Instead, landfill disposal or used for saline soil remediation is recommended.

4. Conclusions

The study developed a Fe^{2+}/SPS–PG method for sludge conditioning and deep dewatering. The individual and combined conditioning processes were compared to investigate the synergetic effects and mechanism of the composite conditioners. The highest SRF and CST reduction efficiencies of 88.5% and 91.5%, respectively, were obtained under the synergetic conditioning of Fe^{2+}/SPS–PG. The protein contents in LB–EPS and in filtrate increased considerably than that in TB–EPS, while polysaccharides contents decreased in LB–EPS and TB–EPS. The destruction of EPS resulted in a decrease of bound water content from 2.60 g/g DS initially to 0.81 g/g DS. Radical quenching experiment suggests that $SO_4^{\cdot-}$ is the dominant radical and plays a major role in oxidation.

The presence of a large number of ions after Fe^{2+}/SPS oxidation promoted the rapid generation of column–shaped dihydrate phases of $CaSO_4{\cdot}2H_2O$ from the hemihydrate phases of $CaSO_4{\cdot}0.5H_2O$. Newly generated column–shaped dihydrate phases act as skeleton builders, and thus improving sludge dewatering. When 23.5 mg Fe^{2+}/g DS, 100.0 mg SPS/g DS and 259.0 mg PG/g DS were chosen for diaphragm filter press dewatering, 45.7% filter moisture content and 91.7% dewatering efficiency were achieved. Overall, the Fe^{2+}/SPS–PG composite conditioner is a promising candidate to improve sludge dewaterability.

Acknowledgments

The author would like to appreciate the financial support provided by the National Natural Science Foundation of China (51078162), the Research Project of Chinese Ministry of Education (113046A), and the Fundamental Research Funds for the Central Universities (2013TS071). The authors would also like to thank the Analytical and Testing Center of Huazhong University of Science and Technology for providing the facilities for the experimental measurements.

Appendix A. Supplementary data

Supplementary data associated with this article can be found, in the online version, at http://dx.doi.org/10.1016/j.cej.2015.01.122.

References

[1] F.Y. García Becerra, E.J. Acosta, D.G. Allen, Alkaline extraction of wastewater activated sludge biosolids, Bioresour. Technol. 101 (2010) 6983–6991.
[2] M. Raynaud, J. Vaxelaire, J. Olivier, E. Dieude-Fauvel, J.C. Baudez, Compression dewatering of municipal activated sludge: effects of salt and pH, Water Res. 46 (2012) 4448–4456.
[3] D. Mowla, H.N. Tran, D.G. Allen, A review of the properties of biosludge and its relevance to enhanced dewatering processes, Biomass Bioenergy 58 (2013) 365–378.
[4] M. Ruiz-Hernando, G. Martinez-Elorza, J. Labanda, J. Llorens, Dewaterability of sewage sludge by ultrasonic, thermal and chemical treatments, Chem. Eng. J. 230 (2013) 102–110.
[5] K. Hii, S. Baroutian, R. Parthasarathy, D.J. Gapes, N. Eshtiaghi, A review of wet air oxidation and thermal hydrolysis technologies in sludge treatment, Bioresour. Technol. 155 (2014) 289–299.
[6] A. Ayol, Enzymatic treatment effects on dewaterability of anaerobically digested biosolids – I: Performance evaluations, Process Biochem. 40 (2005) 2427–2434.
[7] E. Neyens, J. Baeyens, M. Weemaes, B. De heyder, Pilot-scale peroxidation (H_2O_2) of sewage sludge, J. Hazard. Mater. 98 (2003) 91–106.
[8] E. Neyens, J. Baeyens, R. Dewil, B. De heyder, Advanced sludge treatment affects extracellular polymeric substances to improve activated sludge dewatering, J. Hazard. Mater. 106 (2004) 83–92.
[9] T.H. Kim, S.R. Lee, Y.K. Nam, J.C. Yang, M. Lee, Disintegration of excess activated sludge by hydrogen peroxide oxidation, Desalination 246 (2009) 275–284.
[10] H. Liu, J. Yang, Y. Shi, Y. Li, S. He, C. Yang, H. Yao, Conditioning of sewage sludge by Fenton's reagent combined with skeleton builders, Chemosphere 88 (2012) 235–239.
[11] A. Mustranta, L. Viikari, Dewatering of activated sludge by an oxidative treatment, Water Sci. Technol. 28 (1993) 213–221.
[12] E. Neyens, J. Baeyens, A review of classic Fenton's peroxidation as an advanced oxidation technique, J. Hazard. Mater. 98 (2003) 33–50.
[13] C. Liang, I.L. Lee, I.Y. Hsu, C.P. Liang, Y.L. Lin, Persulfate oxidation of trichloroethylene with and without iron activation in porous media, Chemosphere 70 (2008) 426–435.
[14] G. Zhen, X. Lu, Y. Zhao, X. Chai, D. Niu, Enhanced dewaterability of sewage sludge in the presence of Fe(II)-activated persulfate oxidation, Bioresour. Technol. 116 (2012) 259–265.
[15] G. Zhen, X. Lu, Y. Li, Y. Zhao, B. Wang, Y. Song, X. Chai, D. Niu, X. Cao, Novel insights into enhanced dewaterability of waste activated sludge by Fe(II)-activated persulfate oxidation, Bioresour. Technol. 119 (2012) 7–14.
[16] Y. Shi, J. Yang, W. Mao, Y. Li, X. Xu, H. Zhang, W. Yu, Y. Li, C. Yang, Influence of Fe^{2+}-sodium persulfate on extracellular polymeric substances and dewaterability of sewage sludge, Desalin. Water Treat. (2013) 1–9.
[17] J. Zall, N. Galil, M. Rehbun, Skeleton builders for conditioning oily sludge, Journal (Water Pollut. Control Fed.) 59 (1987) 699–706.
[18] J. Benítez, A. Rodríguez, A. Suárez, Optimization technique for sewage sludge conditioning with polymer and skeleton builders, Water Res. 28 (1994) 2067–2073.
[19] Y.Q. Zhao, Enhancement of alum sludge dewatering capacity by using gypsum as skeleton builder, Colloids Surf. Physicochem. Eng. Aspects 211 (2002) 205–212.
[20] Y. Qi, K.B. Thapa, A.F.A. Hoadley, Benefit of lignite as a filter aid for dewatering of digested sewage sludge demonstrated in pilot scale trials, Chem. Eng. J. 166 (2011) 504–510.
[21] H. Luo, X.A. Ning, X. Liang, Y. Feng, J. Liu, Effects of sawdust-CPAM on textile dyeing sludge dewaterability and filter cake properties, Bioresour. Technol. 139 (2013) 330–336.
[22] G.H. Yu, P.J. He, L.M. Shao, P.P. He, Stratification structure of sludge flocs with implications to dewaterability, Environ. Sci. Technol. 42 (2008) 7944–7949.
[23] X.Y. Li, S.F. Yang, Influence of loosely bound extracellular polymeric substances (EPS) on the flocculation, sedimentation and dewaterability of activated sludge, Water Res. 41 (2007) 1022–1030.
[24] B. Frølund, R. Palmgren, K. Keiding, P.H. Nielsen, Extraction of extracellular polymers from activated sludge using a cation exchange resin, Water Res. 30 (1996) 1749–1758.
[25] M. DuBois, K.A. Gilles, J.K. Hamilton, P.A. Rebers, F. Smith, Colorimetric method for determination of sugars and related substances, Anal. Chem. 28 (1956) 350–356.
[26] N. Katsiris, A. Kouzeli-Katsiri, Bound water content of biological sludges in relation to filtration and dewatering, Water Res. 21 (1987) 1319–1327.

[27] D.J. Lee, S.F. Lee, Measurement of bound water content in sludge: the use of differential scanning calorimetry (DSC), J. Chem. Technol. Biotechnol. 62 (1995) 359–365.
[28] H. Zhang, J. Yang, W. Yu, S. Luo, L. Peng, X. Shen, Y. Shi, S. Zhang, J. Song, N. Ye, Y. Li, C. Yang, S. Liang, Mechanism of red mud combined with Fenton's reagent in sewage sludge conditioning, Water Res. 59 (2014) 239–247.
[29] C. Liang, C.J. Bruell, M.C. Marley, K.L. Sperry, Persulfate oxidation for in situ remediation of TCE. I. Activated by ferrous ion with and without a persulfate–thiosulfate redox couple, Chemosphere 55 (2004) 1213–1223.
[30] B. Jin, B.-M. Wilén, P. Lant, Impacts of morphological, physical and chemical properties of sludge flocs on dewaterability of activated sludge, Chem. Eng. J. 98 (2004) 115–126.
[31] G.P. Anipsitakis, D.D. Dionysiou, Radical generation by the interaction of transition metals with common oxidants, Environ. Sci. Technol. 38 (2004) 3705–3712.
[32] C. Liang, H.W. Su, Identification of sulfate and hydroxyl radicals in thermally activated persulfate, Ind. Eng. Chem. Res. 48 (2009) 5558–5562.
[33] J. Yang, W. Liu, L. Zhang, B. Xiao, Preparation of load-bearing building materials from autoclaved phosphogypsum, Constr. Build. Mater. 23 (2009) 687–693.
[34] E.A. Abdel-Aal, M.M. Rashad, H. El-Shall, Crystallization of calcium sulfate dihydrate at different supersaturation ratios and different free sulfate concentrations, Cryst. Res. Technol. 39 (2004) 313–321.